JOURNAL OF MATERIALS SCIENCE 29 (1994) 218–226

Precipitate structure in a Cu–Ni–Si alloy

S. A. LOCKYER, F. W. NOBLE
Department of Materials Science and Engineering, University of Liverpool, Liverpool L69 3BX, UK

The precipitates responsible for the age-hardening effect in dilute Cu–Ni–Si alloys based on Cu2NiSi have been studied using transmission electron microscopy. The work has confirmed the findings of an earlier study by Teplitskiy *et al.*, which showed that the precipitates formed as discs on {1 1 0} planes and indicated that they had a structure which corresponded to that of δ-Ni_2Si. The orientation relationship of the precipitate and matrix found in the present work differs from that found in the earlier work, and a high degree of coherency across the precipitate–matrix interface has been shown to exist. In establishing that the precipitate is δ-Ni_2Si, EDX analysis has been employed and ring patterns from extracted precipitates have also been analysed. Absences from such ring patterns which were noted in the earlier work and which were thought to cast doubt on the precipitate identification have been accounted for in terms of preferred orientation effects. At peak strength the deformation of the material is believed to involve Orowan looping around the precipitates.

1. Introduction

Cu–Ni–Si alloys with compositions corresponding approximately to Cu–2 at% Ni–1 at% Si exhibit a significant age-hardening effect. Typically such alloys are aged at about 450 °C after quenching from the solution treatment temperature, and tensile strengths in the range 600 to 800 MPa are attainable depending upon ageing time and whether or not the alloy is cold-worked prior to ageing. Age-hardening in this system was first investigated by Corson [1, 2] and the precipitating phase responsible for the hardening was identified as δ-Ni_2Si on the basis of a quasi-binary section of the Cu–Ni–Si ternary diagram. This identification was subsequently disputed: Okamoto [3, 4] claimed that the quasi-binary section in question was incorrect and identified the precipitating phase in aged alloys as γ-Ni_5Si_2; Robertson *et al.* [5] found that particles extracted on to replicas from aged material appeared to be β-Ni_3Si.

The application of transmission electron microscopy (TEM) to thin films of the aged material (in conjunction with X-ray diffraction and hardness measurements) by Dies *et al.* [6] showed that the precipitated phase was formed in a well-defined crystallographic orientation with respect to the matrix, that its crystal structure was orthorhombic, or of higher symmetry, and that its lattice parameter was about four times that of copper. Dies *et al.* compared X-ray diffraction patterns obtained from aged material with those obtained from conventional binary Ni–Si intermetallic compounds, and on this basis concluded that the structure of the precipitate formed in aged material did not correspond to any of the known intermetallic nickel–silicon compounds. Further TEM work by Teplitskiy *et al.* [7] yielded results which indicated that the structure of the precipitated phase in the maximum strengthening range of the alloys is δ-Ni_2Si, though these authors considered that diffraction patterns obtained from precipitates extracted from material aged for 4 h at 550 °C did not fully support the contention that this phase was formed in the early stages of precipitation.

In the present work the structure, composition and morphology of the precipitate in commercial material corresponding to Cu2NiSi has been investigated as part of a study of the fatigue behaviour of the material. The ageing temperature employed was 450 °C (the commercially recommended ageing temperature) and various ageing times have been investigated. The characteristics of the precipitate have been established by electron microscopy and correlated with the strength of the alloy. High-resolution electron microscopy (HREM) has also been used to supplement conventional TEM.

2. Experimental procedure

The alloy used in this investigation was supplied by Columbia Metals (UK) and is marketed as Colsibro. Its specified composition is 1.6–2.4 wt% Ni and 0.4–0.8 wt% Si, the balance being Cu. In the as-received condition the alloy was in the form of 12.5 mm bar and had been solution-treated, cold-worked and aged. For the purposes of this work the material was again solution-treated for 2 h at 800 °C under an $N_2 + H_2$ atmosphere, water-quenched and then aged (without prior cold work) at 450 °C under an $N_2 + H_2$ atmosphere for various periods up to 1000 h prior to air cooling. Age-hardening was monitored using Vickers hardness tests.

For thin-film TEM examination, material in the form of 3 mm diameter rods was cut into discs and ground to a thickness of 0.3 mm prior to thinning in a Struers Tenupol using a Struers D2 electrolyte at

0022–2461

room temperature. The thinning conditions were a voltage of 6–8 V and a flow rate setting of 5.5. Extraction replicas were obtained from surfaces which had been electropolished in the same solution as that used for thinning. Most of the electron microscopy for this study was carried out using a Philips EM400T operating at 120 kV, but for energy-dispersive X-ray (EDX) analysis a Jeol 2000 FX was used; HREM images of the precipitates were obtained using a Jeol 2000 EX. Both the latter microscopes were operated at 200 kV.

3. Results

3.1. Age-hardening response and precipitate morphology

The effect of ageing for times between 1 and 1000 h on the hardness of the material is shown in Fig. 1. The peak hardening effect occurs after ageing for about 25 h and the hardness decreases continuously at longer ageing times. The precipitates are not visible optically but are visible at high magnification by TEM. Bright-field electron micrographs of the precipitates are shown in Fig. 2 for ageing times of 2 h (Fig. 2a), 100 h (Fig. 2b) and 1000 h (Fig. 2c). The precipitates in Fig. 2a and 2b are associated with considerable strain contrast but this was less in evidence in the 1000 h aged material (Fig. 2c). In the latter condition the precipitate morphology was visible more clearly, the precipitates appearing as rods in some cases and discs in others.

Precipitates formed during ageing for 750 h were imaged under dark-field conditions, and a dark-field micrograph is shown in Fig. 3a. This micrograph was obtained from a foil oriented such that the incident beam was parallel to $[0\,0\,1]_m$ (m signifying matrix). The diffraction pattern corresponding to this foil orientation is shown in Fig. 3b. The (bright) matrix spots correspond to reflections from $\{2\,0\,0\}_m$ and $\{2\,2\,0\}_m$; the precipitate spots are elongated in either the $[1\,1\,0]_m$ or the $[1\,\bar{1}\,0]_m$ direction. Fig. 3a was obtained using a large aperture centred on one of the precipitate

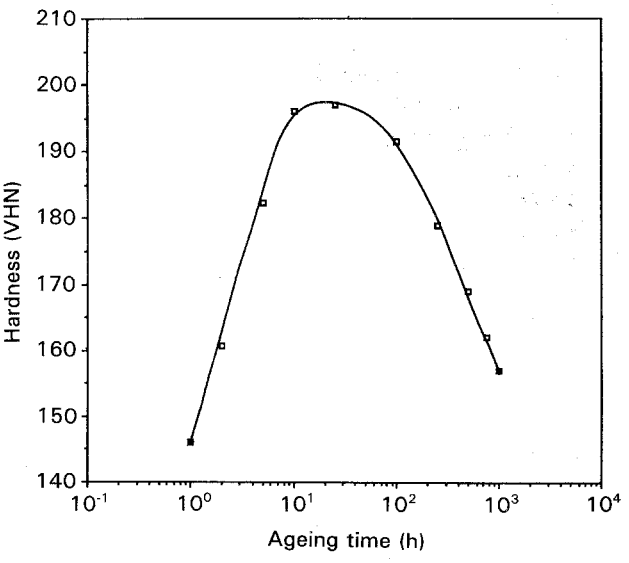

Figure 1 Ageing response of the material at 450 °C.

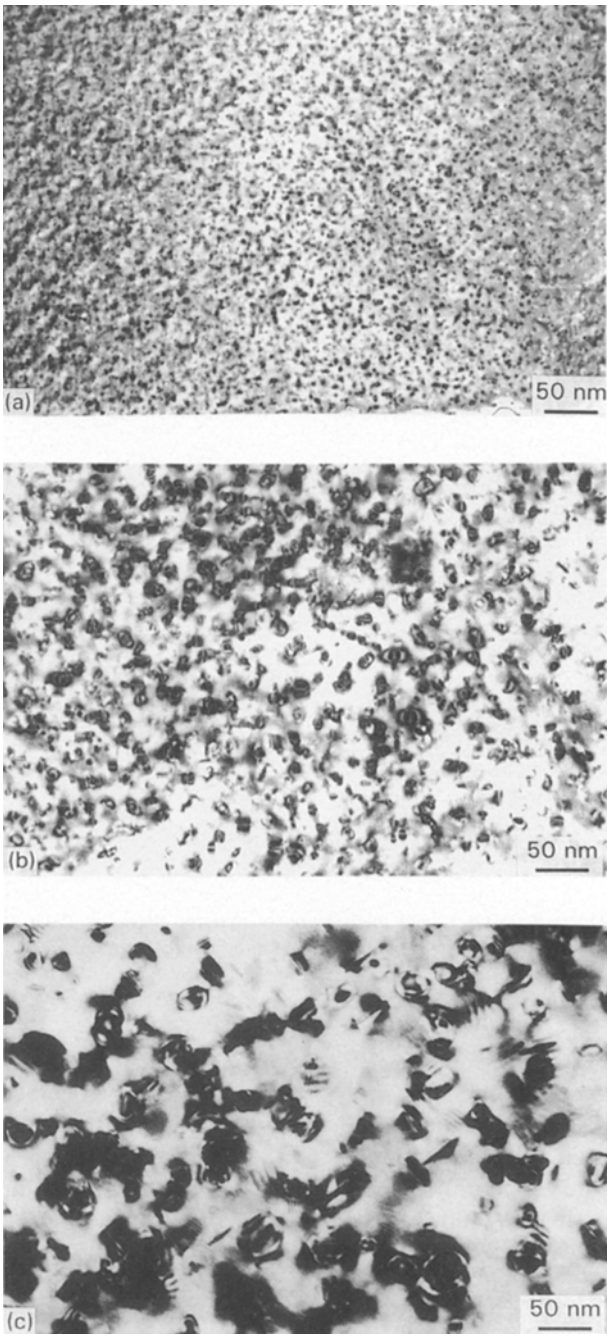

Figure 2 TEM micrographs showing the appearance of the precipitates after different ageing times: (a) 2 h, (b) 100 h, (c) 1000 h.

reflections which lies midway between 0 0 0 and each $2\,2\,0_m$ reflection (labelled A in Fig. 3b). Two sets of rod-shaped images of the precipitates can be seen, at right-angles to each other and elongated in the two $\langle 1\,1\,0\rangle_m$ directions orthogonal to the beam direction. Other fainter, disc-shaped precipitates are visible in the background. These images are consistent with the precipitates having formed as discs on $\{1\,1\,0\}_m$ planes, as reported by Teplitskiy *et al.* [7]. The discs lie on the $(1\,1\,0)_m$ and $(1\,\bar{1}\,0)_m$ planes parallel to the beam and so appear as rods.

Dark-field images were also obtained from foils orientated with the beam direction parallel to $\langle 1\,1\,1\rangle_m$. One of these, obtained from material aged for 750 h, is shown in Fig. 4a; the diffraction pattern corresponding to this orientation, but for material

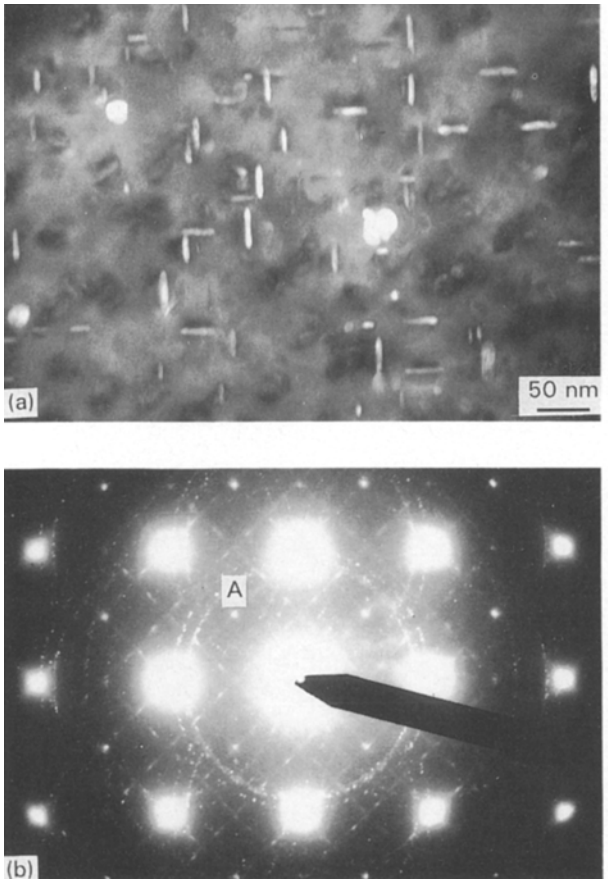

Figure 3 (a) Dark-field micrograph of material aged for 750 h at 450 °C; imaged using the $0\,2\,0_{ppt}$ reflection marked A in the pattern shown in (b). (b) Diffraction pattern for the foil orientation in (a); beam direction parallel to $\langle 0\,0\,1 \rangle$ matrix.

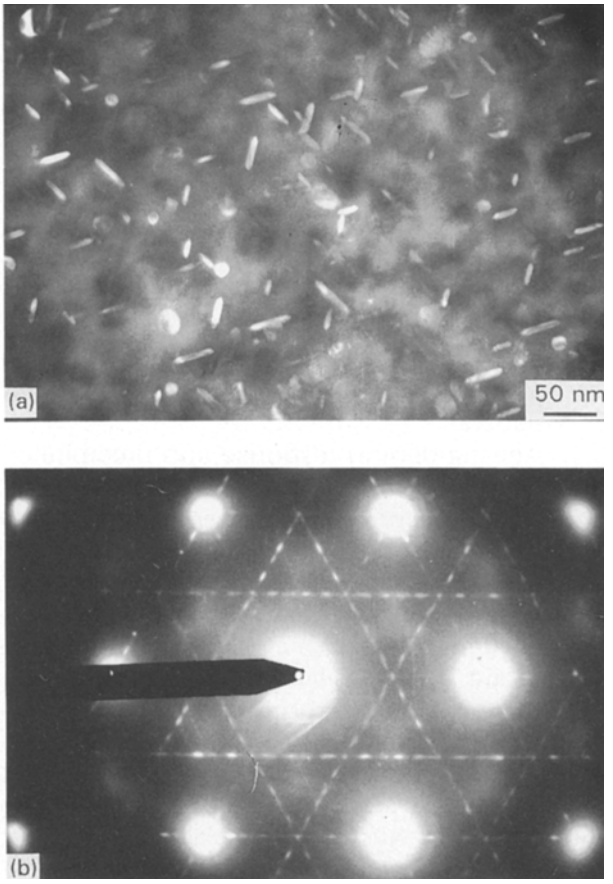

Figure 4 (a) Dark-field micrograph corresponding to the orientation in (b); beam direction parallel to $\langle 1\,1\,1 \rangle$ matrix. (b) Diffraction pattern for the foil orientation in (a) but obtained from material aged for 100 h at 450 °C.

aged for 100 h, is shown in Fig. 4b. The precipitate discs which lie on the three $\{1\,1\,0\}_m$ planes at 120° to each other and parallel to the beam direction give three superimposed diffraction patterns, the spots in each being elongated normal to one of the $\{1\,1\,0\}_m$ planes. The micrographs indicate that after this ageing time (750 h) the disc diameter is 34 nm and the thickness is 6 nm. The variation of precipitate size with ageing time measured from dark-field micrographs is shown in Fig. 5.

High-resolution electron microscopy was also used to image the precipitates formed after ageing for 2 and 100 h. The results obtained are shown in Fig. 6a and b, respectively. The plane of the foil is $\{0\,0\,1\}_m$ in each case and the images corresponding to the $\{0\,2\,0\}_m$ planes are indicated. In both cases the precipitates show evidence of a periodicity along their apparent length in the form of regularly repeated fringes; in the 100 h aged material these fringes are associated with bright spots. In both cases the periodicity corresponds approximately to twice that of the spacing of $\{1\,1\,0\}_m$. There is also evidence of periodicity in the transverse direction but it is less well defined: it corresponds to about $4 \times d_{0\,0\,2}$ Cu, i.e. 0.72 nm (~ half the precipitate width for the 2 h aged material; ~ 1/3 to 1/4 the precipitate width for the 100 h aged material). Strain contrast associated with the precipitates was visible after each ageing treatment, indicating that most retain some degree of coherency after 100 h ageing.

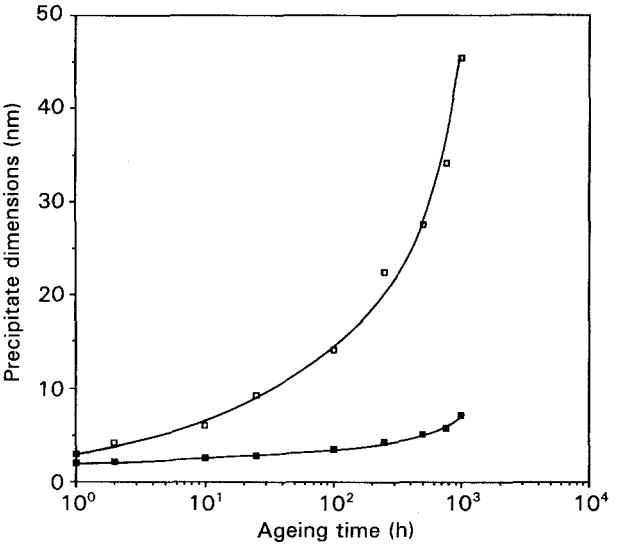

Figure 5 Variation of ((□) diameter and (■) thickness) of precipitates with ageing time at 450 °C.

3.2. Interpretation of the diffraction patterns

3.2.1. Selected-area patterns

Fig. 7a–d show selected-area diffraction patterns obtained from material aged for 2, 100, 750 and 1000 h, respectively. The incident beam is parallel to $\langle 0\,0\,1 \rangle_m$ in each case. In addition to the diffraction spots there are diffraction rings, which are especially

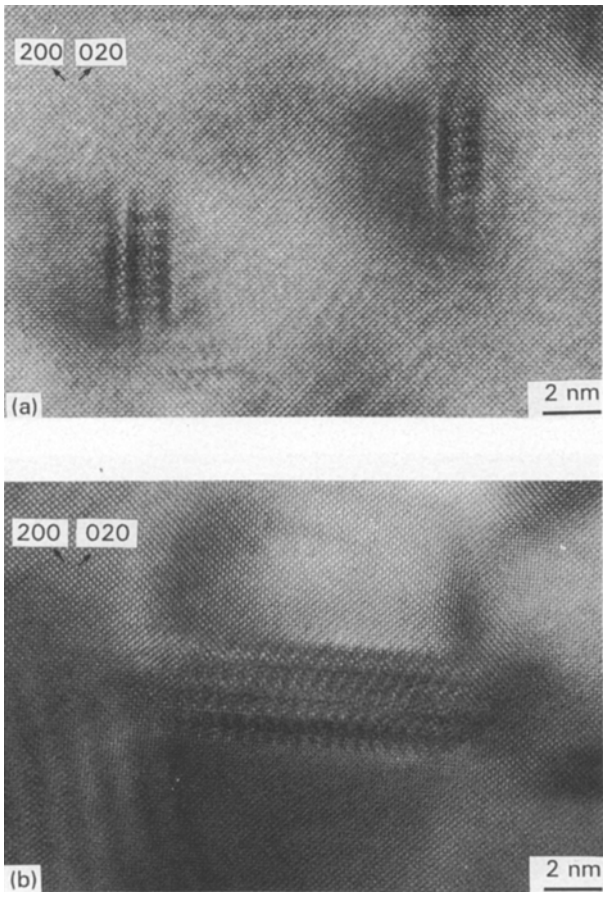

Figure 6 HREM micrographs of a foil orientated with the beam direction along ⟨0 0 1⟩: (a) 2 h, (b) 100 h.

prominent in the 100 h aged sample. The significance of the rings will be discussed later.

In the 2 h aged condition the precipitates give rise to the distinct diffraction spots in positions equivalent to A in Fig. 3b above, i.e. almost exactly mid-way between 0 0 0 and the 2 2 0 matrix reflections, and there are many other less distinct spots streaked in either of the two $\langle 1\,1\,0\rangle_m$ directions orthogonal to the beam. The precipitate reflections in the pattern from 100 h aged material give much sharper spots, allowing the faint grid pattern of precipitate reflections visible in Fig. 7a to be resolved into individual, streaked spots. The diffraction pattern for the 1000 h aged material shows still more spots but the general features of the pattern remain unchanged.

The diffraction patterns are complicated by the fact that while the incident beam gives rise to two sets of precipitate reflections, corresponding to the precipitates on $(1\,1\,0)_m$ and $(1\,\bar{1}\,0)_m$, each of the bright matrix reflections gives rise to two more sets, centred on that reflection. The near colinearity of the precipitate spots from these different sources in the direction of streaking indicates that the precipitate and matrix structures have similar periodicities normal to that direction. When the multiplicity of patterns is allowed for, the pattern due to a single precipitate orientation can be extracted. It corresponds to the one shown schematically in Fig. 8 and is similar to that depicted in Teplitskiy *et al.* [7] except that in that representation the precipitate spots between $0\,0\,0_m$ and $2\,2\,0_m$ referred to above are not included. Fig. 8 is, in fact, a computer

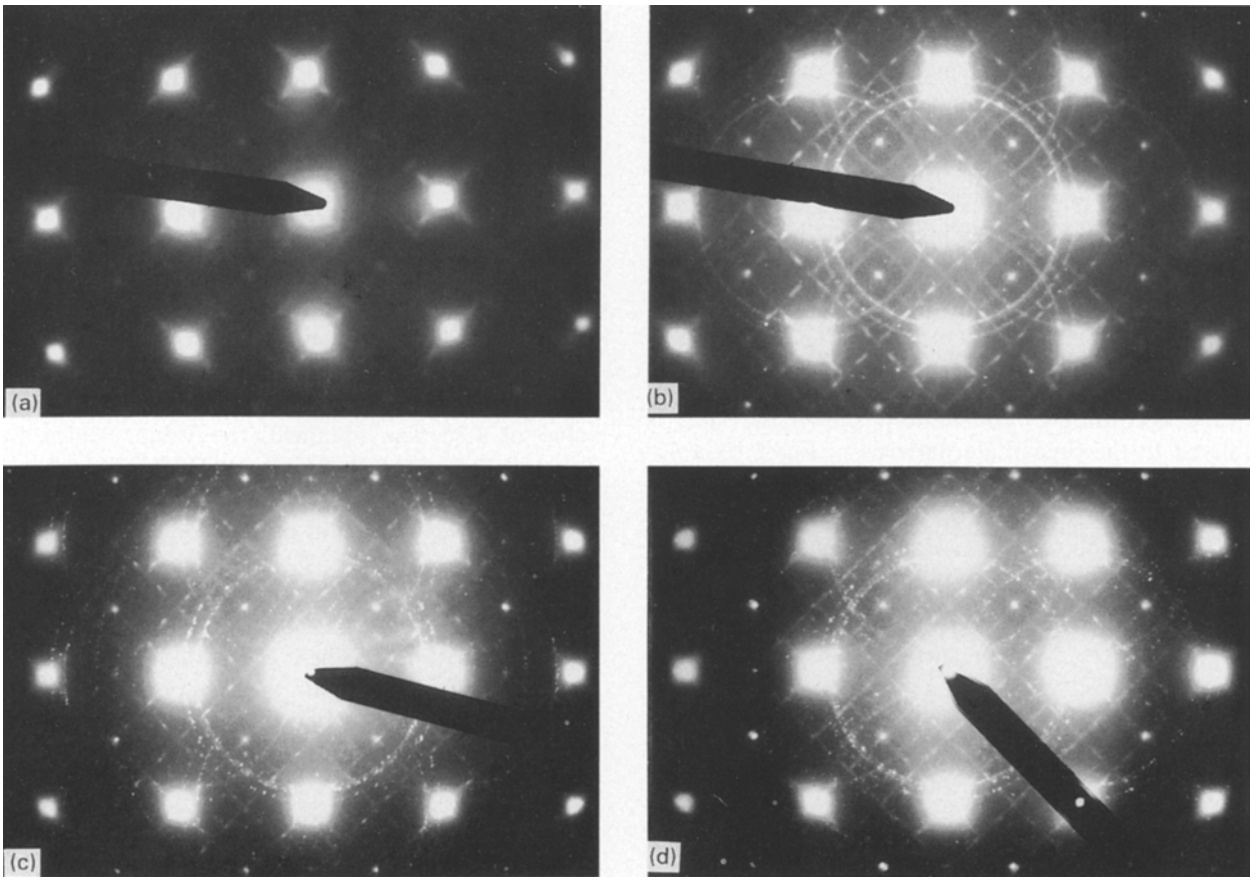

Figure 7 Selected-area diffraction patterns from material aged for different times (beam direction along ⟨0 0 1⟩ in each case): (a) 2 h, (b) 100 h, (c) 750 h, (d) 1000 h.

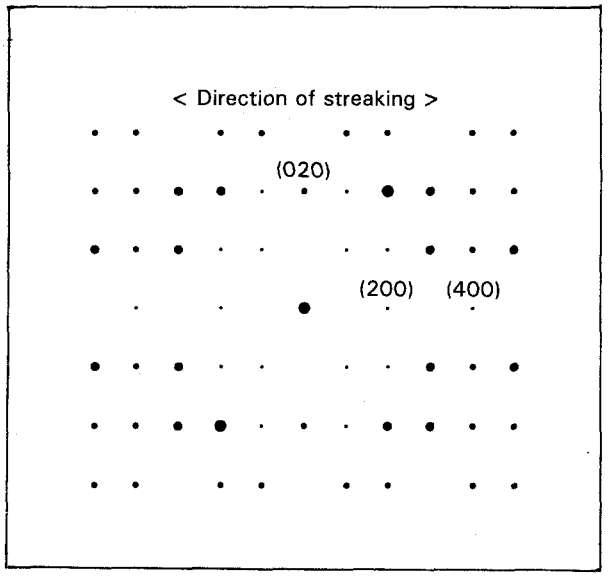

Figure 8 Simulated diffraction pattern for δ-Ni_2Si. The pattern corresponds to one of the precipitate patterns in Fig. 7 with the effects of double diffraction removed, rotated through 45°.

simulation of a pattern produced by δ-Ni_2Si. The indexing is explained below, as are the size differences between the spots.

The diffraction patterns in Fig. 7 show that an orientation relationship clearly exists between the precipitate and the matrix. The spacing of the precipitate spots in the $\langle 1\,1\,0\rangle_m$ direction normal to the streaking shows that the interplanar spacing in the precipitate is approximately equal to twice the spacing of the (1 1 0) matrix planes, as inferred from the HREM images. The spot spacing in the orthogonal direction indicates that the interplanar spacing in this direction is approximately 1.4 times larger again. The latter figure appeared to be independent of ageing time and hence precipitate size. It corresponds to the a/b ratio of the orthorhombic δ-Ni_2Si structure found by Toman [8] for which $a = 0.703$ nm, $b = 0.499$ nm and $c = 0.372$ nm ($a/b = 1.4088$). The diffraction pattern is, therefore, consistent with the Ni_2Si structure if the periodicity in the $\langle 1\,1\,0\rangle_m$ direction normal to the streaking is identified with b and that in the orthogonal $\langle 1\,1\,0\rangle_m$ direction with a. Fig. 8 has been indexed accordingly. The pattern shown in Fig. 8 is related to the precipitate patterns in Fig. 7 by a 45° rotation. The spot sizes in Fig. 8 are indications of the expected relative brightness of the different spots based on structure-factor considerations. The orientation relationship implied by the above interpretation of the diffraction patterns is

$$(1\,0\,0)_m \| (0\,0\,1)_{ppt}$$

$$[0\,1\,1]_m \| [0\,1\,0]_{ppt}$$

the habit plane being $(0\,1\,1)_m$.

The diffraction pattern obtained with the incident beam parallel to $[1\,1\,1]_m$ is shown in Fig. 9a for 2 h aged material and in Fig. 9b for 750 h aged material. These patterns are consistent with the δ-Ni_2Si structure and with the above orientation relationship. Although the majority of the precipitate spots in Fig. 9b

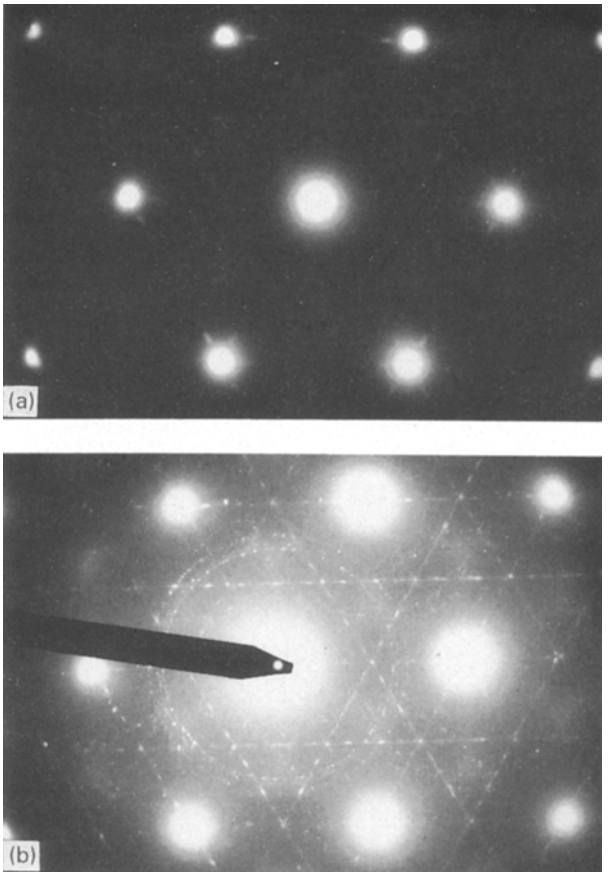

Figure 9 Selected-area diffraction patterns from material aged for different times (beam direction along $\langle 1\,1\,1\rangle$ in each case): (a) 2 h, (b) 750 h.

are streaked in one of three different directions (corresponding to discs on the three $\{1\,1\,0\}$ planes parallel to the beam) there are spots at the vertices of the innermost hexagon formed by the intersections of these patterns which do not appear to be streaked. These spots lie at points apparently midway between 0 0 0 and the $2\,2\,0_m$ reflections and do not belong to any of the three prominent precipitate patterns. These can be identified as reflections from the $0\,2\,0_{ppt}$ planes of the precipitates formed on the three $\{1\,1\,0\}_m$ planes which are not parallel to the beam. Using these spots in conjunction with the $0\,2\,2_{ppt}$ reflections enabled the b/c ratio for the precipitate to be calculated. An average value of 1.38 was obtained: the value yielded by Toman's data for δ-Ni_2Si is 1.34. This difference will be considered later.

In the $0\,0\,1_m$ diffraction pattern for the 750 h aged alloy in Fig. 3b and the $1\,1\,1_m$ pattern for the 750 h aged material in Fig. 9b there are additional spots which correspond to forbidden reflections ($0\,1\,1_{ppt}$ in Fig. 9b, for example). These effects may be attributed to double diffraction within the precipitates, the additional spots only appearing when the precipitates have grown to an appreciable size and the spots are sharper as a result of streaking having decreased.

3.2.2. The ring patterns

The ring patterns visible on the conventional selected-area patterns in Fig. 7 were also obtained by Teplitskiy

et al. [7], who attributed them to diffraction from precipitate particles "washed out onto the surface of the foil" during thinning. The existence of such precipitates was checked in the present work by examining a foil surface in SEM mode and also by taking replicas from the surface of electropolished samples of 100 h aged material and 1000 h aged material. An SEM micrograph of the foil surface (100 h aged sample) is shown in Fig. 10a; the precipitates extracted on the replica are shown in Fig. 10b. The profusion of discs on the replica supports the claim of Teplitskiy *et al.* and is in line with similar effects in other precipitate containing alloys [9, 10]. The precipitates on the replicas produced ring diffraction patterns (Figs 11a and b) in which there were two intense inner rings which corresponded to those in the diffraction patterns obtained from the foils (Fig. 7). The outermost of these two rings was identified by Teplitskiy *et al.* as being due to (0 0 2) δ-Ni_2Si, and the present results are in agreement with this attribution. The ring patterns, from the replicas taken from both 100 h and 1000 h aged material, could be indexed according to the δ-Ni_2Si structure, and in the 1000 h aged case discrete identifiable spots were observed in positions in which rings could be expected but no complete ring had developed. The results from the ring patterns from the replicas are shown in Table I, and those from the foils in Table II. Table I lists the rings identified after 1000 h ageing, and indicates which rings were also present in patterns obtained after 100 h ageing.

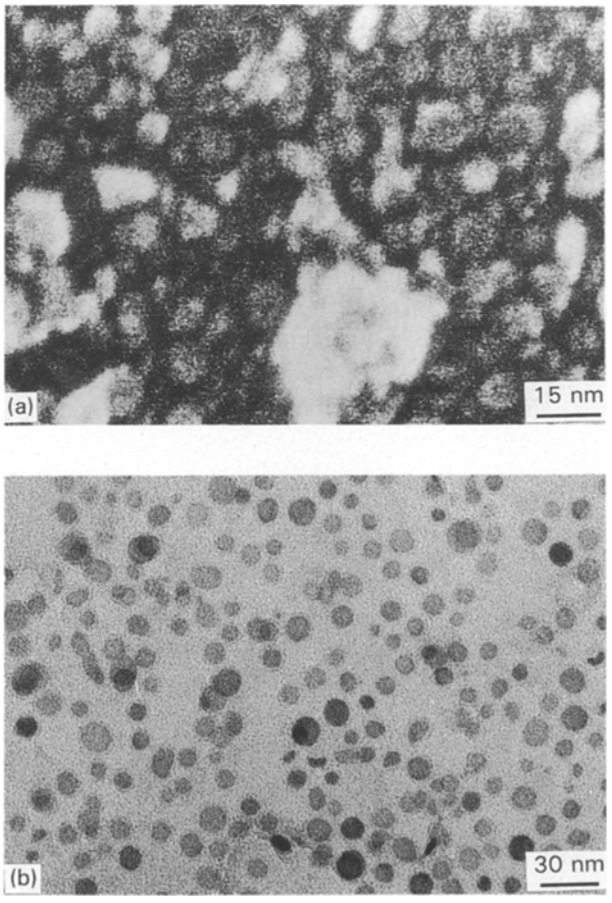

Figure 10 (a) Surface of thin foil of material aged for 100 h viewed using the STEM facility in SEM mode. (b) Precipitates extracted on a replica obtained from an electropolished surface of a 100 h aged specimen.

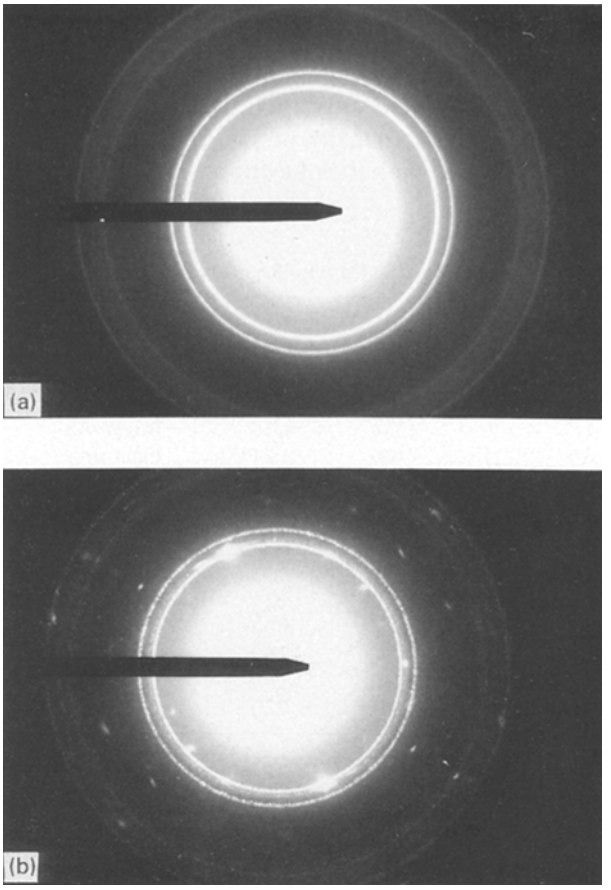

Figure 11 Ring patterns obtained from precipitates extracted on to replicas taken from material aged for (a) 100 h and (b) 1000 h.

TABLE I Ratios calculated from replicas using the inner 0 2 0 ring (material aged for 1000 h)

Measured ratio	Theoretical ratio	Possible indices	Relative intensity
1.000	1.000	0 2 0[a]	Faint ring
0.912	0.911	2 1 1	Faint spot
0.861	0.850	3 1 0	Bright spot
0.833	0.831	0 2 1[a]	Bright ring
0.816	0.815	2 2 0[a]	Bright ring
0.799	0.797	1 2 1[a]	Spotty ring
0.742	0.745	0 0 2[a]	Bright ring
0.686	0.685	3 2 0[a]	Faint spot
0.646	0.649	1 3 0[a]	Bright spot/faint ring
0.625	0.622	3 2 1	Faint spot
0.603	0.602	2 3 0	Bright spot
0.562	0.559	3 1 2	Bright spot
0.550	0.550	2 2 2[a]	Faint ring
0.487	0.492	1 4 0	Faint ring
0.464	0.461	4 3 1	Bright spot/faint ring
0.439	0.440 or 0.439	1 2 3 or 3 0 3	Medium ring
0.407	0.406	4 3 2	Faint ring

[a] Also present in patterns obtained after 100 h ageing.

3.3. Compositional analysis

An attempt was made to estimate the composition of the precipitates in 100 h and 1000 h aged material using the EDX technique on thin foils and analysing

the results according to the method of Cliff *et al.* [11]. In this type of plot, shown in Fig. 12, the true composition is obtained by extrapolating out the contribution of the matrix to the analysis. The extrapolation indicates that there is virtually no Cu in the precipitates and is consistent with their having a composition close to Ni_2Si. The results show a variation in composition from precipitate to precipitate, the deviations from the stoichiometric composition mainly being on the silicon-rich side. Attempts were made to analyse the precipitates extracted on carbon replicas, but there were indications that these results were unduly affected by silicon contamination in the microscope.

TABLE II Ratios calculated from foils using the bright 002 ring

Measured ratio	Theoretical ratio	Possible indices	Relative intensity
100 h ageing			
1.117	1.114	021	Bright ring
1.078	1.066	121	Faint ring
1.000	1.000	002	Medium ring
0.595	0.597	023	Very faint ring
1000 h ageing			
1.119	1.114	021	Spotty ring
1.074	1.066	121	Spotty ring
1.000	1.000	002	Bright spots
0.748	0.738	222	Very faint ring
0.662	0.660	140	Faint ring
0.596	0.597	023	Faint spotty ring

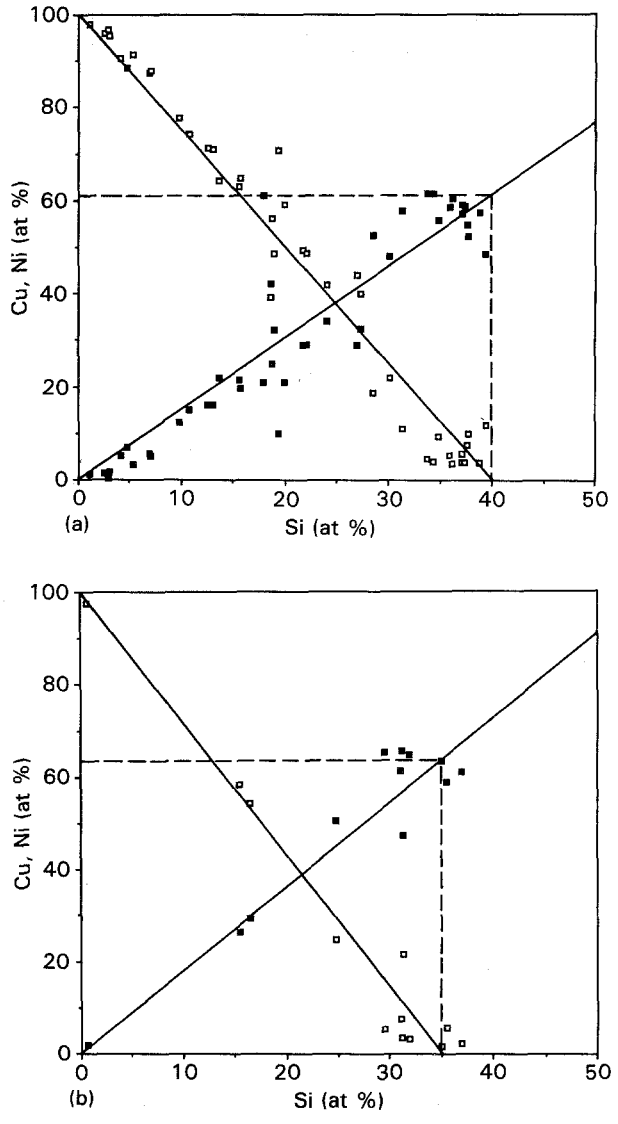

Figure 12 EDX data from precipitates in material aged for (a) 100 h and (b) 1000 h. Analyses performed using foils; (□) Cu, (■) Ni.

4. Discussion

4.1. The coherency of the precipitate

The orientation relationship is such that the $(0\,\bar{1}\,1)_m$ planes lying normal to the $(0\,1\,1)_m$ habit plane are parallel to $(0\,1\,0)_{ppt}$. The similarity in spacing between the (0 1 0) planes in δ-Ni_2Si and alternate (0 1 1) planes in copper (0.499 and 0.512 nm, respectively) suggests the possibility that there is continuity between both these sets of planes across the interface. The lattice parameters indicate that the unrelaxed mismatch involved is 2.6%; the relaxed mismatch should be less than this. The latter can, in principle, be obtained from the appropriate spot spacings in the diffraction patterns obtained from aged material. In practice it is difficult to quantify with sufficient accuracy by direct measurement, though such measurements do indicate a value of less than 2.6%. The mismatch can also be obtained from measurements of the extent to which the double diffraction spots from different matrix-diffracted beams deviate from complete colinearity with spots from the primary precipitate pattern in the rows of precipitate reflections orthogonal to the habit plane – complete colinearity would imply no mismatch. This deviation from colinearity can be seen in Fig. 13 which is an enlargement of Fig. 7b. The $1\,3\,0_{ppt}$ reflection from the incident beam is labelled B; the adjacent spot (labelled C) is a precipitate reflection deriving from the matrix reflection marked X and, relative to X, is $3\,1\,0_{ppt}$. The difference in horizontal separation of these spots relative to the spot spacing corresponding to the $\{1\,1\,0\}_m$ spacing gives the mismatch in question. It is about half the relaxed value, i.e. close to 1%. The value of the *b* lattice parameter for the precipitate indicated by this mismatch is about

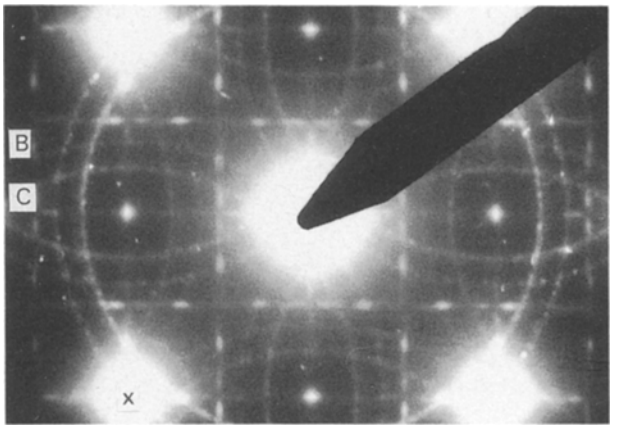

Figure 13 Enlargement of part of Fig. 7b showing displacement of the diffraction spots from colinearity as a result of the slight mismatch between the spacing between {1 1 0} planes in the matrix and the parallel (0 2 0) planes in δ-Ni_2Si.

0.506 nm, compared with the value of 0.499 nm for unconstrained δ-Ni_2Si. Since the a/b ratio indicated by the diffraction pattern is about 1.4, this implies that the a parameter is also larger than the relaxed δ-Ni_2Si value – about 0.708 nm rather than 0.703 nm.

The parallelism of $(1\,0\,0)_m$ and $(0\,0\,1)_{ppt}$ in the orientation relationship and the similar interplanar spacings of these planes in the two crystal lattices (0.362 and 0.372 nm, respectively) suggests that these two planes also may be continuous across the interface. The completely unrelaxed misfit between these planes is about 2.8%. An indication of the relaxed misfit can be obtained from the value for the c parameter given by diffraction patterns analysed above ($b/c = 1.38$, $b = 0.506$ nm). These data yield a value for c of 0.367 nm – indicative of a misfit of about half the unrelaxed value.

On the basis of the above estimates, therefore, the mismatch between precipitate and matrix is of the order of 1% in the b and c directions, which lie in the habit plane, and as such the interface between the precipitate and the habit plane is highly coherent. In the a direction there is no obvious match between the periodicity of the precipitate and the periodicity of the matrix in the parallel $\langle 1\,1\,0\rangle_m$ direction, nor would lattice correspondence in this direction be expected.

4.2. Precipitate structure, composition and orientation relationship

While the orthorhombic structure indicated by the diffraction patterns and the lattice parameter relationships inferred from the selected-area diffraction patterns appear to confirm the identification of the precipitate as δ-Ni_2Si, there are some anomalous features. In general the spot intensities on the diffraction patterns are in agreement with structure-factor calculations but there are exceptions: $2\,1\,0_{ppt}$ in Fig. 7 is of comparable brightness to $3\,1\,0_{ppt}$ although the latter has a structure factor of 15 compared with 0.4 for the former (see Fig. 8). In addition the analysis data indicate that the composition of the precipitate deviates from stoichiometry on the Si-rich side. The former anomaly has not been resolved; the latter may be a consequence of contamination or possibly reflects the ability of silicon to dissolve in δ-Ni_2Si, since silicon is reported to dissolve in the high-temperature θ form of Ni_2Si causing the temperature of the θ–δ transformation to drop from 1214 to 806 °C.

Teplitskiy *et al.* [7] concluded that their ring diffraction patterns did not support the suggestion that the phase precipitated in the early stages of ageing (4 h at 550 °C) was δ-Ni_2Si on the grounds that many of the rings expected to be present in diffraction patterns from precipitates extracted on replicas were missing. However, accepting their contention that the ring-producing precipitates are those washed out on to the surface of electropolished material then, given the disc shape of the precipitates, they would be expected to lie flat on the surface of the material and also on replicas taken from that surface (see Fig. 10b). There would therefore be a strong preferred orientation, with $(1\,0\,0)_{ppt}$ (the flat surface of the disc) parallel to the surface of the replica. In these circumstances only planes making large angles with $(1\,0\,0)_{ppt}$ would be expected to diffract and the absence of reflections such as 1 1 1, 2 1 1, 3 2 2, etc. is to be anticipated. Conversely rings corresponding to 0 0 2 and 0 2 1 reflections should arise and rings corresponding to 1 2 1 and 1 4 0 might also be present – the latter four reflections were indeed reported by Teplitskiy *et al.* The preferred orientation of the discs should also manifest itself in ring absences from the ring patterns obtained from foils and, as Table II shows, this is the case. It is suggested, therefore, that the ring absences in the annular patterns are a consequence of the preferred orientation of the precipitates on the replica and do not constitute evidence that the structure of the precipitate is inconsistent with δ-Ni_2Si. The fact that spots corresponding to individual intensity maxima were observed at "missing" ring positions supports this view.

It is also worth noting that in Dies *et al.* [6], although it was claimed that no match was found between the X-ray diffraction data and the existing data for binary Ni–Si compounds, the data quoted by these authors are in good agreement with the data for Ni_2Si given by Toman [8]. The structure-factor values given by Toman indicate that the δ-Ni_2Si reflection with highest intensity should be 0 0 2, followed by 3 0 1. The spacings of these planes correspond well with the values given by Teplitskiy *et al.* [7] for the two most intense reflections (surprisingly so, given the unrelaxed value of c inferred from the electron diffraction data analysed above), and the other two spacings quoted agree well with those for $(3\,2\,0)_{ppt}$ and $(1\,4\,0)_{ppt}$.

The orientation relationship proposed here differs from that put forward by Teplitskiy *et al.* in that while they too found $(1\,0\,0)_m \| (0\,0\,1)_{ppt}$ they give $[3\,1\,0]_{ppt} \| [0\,3\,1]_m$, whereas the diffraction patterns obtained here suggest that the parallelism between $[0\,1\,0]_{ppt}$ and $[0\,1\,1]_m$ provides the most accurate description of the orientation relationship. The relationship found here is similar to that proposed for the early stages of precipitation in Cu–Be alloys [12, 13] though the habit plane in that case is $\{1\,0\,0\}_m$ rather than $\{1\,1\,0\}_m$.

4.3. The strength of the material

The peak hardness, 197 HV, corresponds to a 0.2% proof stress of 610 MPa – a net strength increase due to the precipitates of about 500 MPa which implies an increase in shear strength of about 200 MPa, depending on the value chosen for the Taylor orientation factor. It is difficult to believe that the deformation of peak-aged material involves the Ni_2Si precipitates shearing with the matrix, given the complexity of the crystal structure and the orientation relationship of the precipitates with the matrix. Slip on a specific $\{1\,1\,1\}\ \langle 1\,1\,0\rangle$ matrix slip system would require precipitates in one orientation to shear in the b direction, in another in the a direction and in the other four in a direction close to $\{2\,3\,6\}_{ppt}$. While this may not be impossible it does not seem likely, and it seems reasonable to assume that the precipitates will act as impen-

etrable obstacles to dislocation movement. As such the deformation would appear to involve Orowan looping, though the coherency strains and the geometry associated with six differently oriented precipitates intersecting the slip plane obviously complicate the matter. If, for simplicity, the precipitate size is expressed as an equivalent diameter, a value of about 5 nm is found for the peak-aged material, and thin-foil measurements indicate a corresponding interparticle spacing in the slip plane, λ, of about 40 nm [14]. Taking the Orowan stress as $\mu\mathbf{b}/\lambda$, where μ is the shear modulus and **b** the Burgers vector, gives a shear stress increment for the peak-aged material of $\mu/160$ or about 300 MPa. Although the calculation is rough, the magnitude of the stress is consistent with the suggestion that the peak strength is determined by the Orowan mechanism.

5. Conclusions

1. The precipitate formed in alloys of the type Cu2NiSi has a structure corresponding to δ-Ni_2Si, which is orthorhombic. The precipitates formed in the early stages of ageing (1 h at 450 °C) appear to have this structure, as do the precipitates in the long-term (1000 h) aged material.

2. The lattice parameters of the precipitate structure indicated by electron diffraction measurements are consistent with those obtained for pure δ-Ni_2Si by Toman [8] using X-ray diffraction, though there is an indication that coherency with the matrix causes a slight increase in the *b* parameter and a decrease in the *c* parameter within the precipitate.

3. The precipitates form as discs on $\{1\,1\,0\}$ matrix planes. The orientation relationship is

$$(1\,0\,0)_m \| (0\,0\,1)_{ppt}$$
$$[0\,1\,1]_m \| [0\,1\,0]_{ppt}$$

4. The peak strength occurred after 25 h ageing, at which point the average precipitate diameter and thickness were 9.30 and 2.84 nm, respectively.

Acknowledgements

The authors would like to thank Dr C. J. Kiely and Professor R. C. Pond for many useful discussions. They would also like to thank Mr M. Excell of Columbia Metals for assistance with the provision of material. Finally they would like to thank R. Devenish for the help he provided in obtaining the HREM images and the compositional data.

References

1. M. G. CORSON, *Trans. AIME* (1927) 435.
2. *Idem, Iron Age* **119** (1927) 421.
3. M. OKAMOTO, *Trans. Inst. Met. Jpn* **3**(9) (1939) 336.
4. *Idem, ibid.* **3**(10) (1939) 365.
5. W. D. ROBERTSON, E. G. GRENIER and V. F. NOLE, *Trans. Met. Soc. AIME* **221** (1961) 503.
6. K. DIES, U. HEUBNER and P. WINCIERZ, *Z. Metallkde* **57** (1966) 521.
7. M. D. TEPLITSKIY, A. K. NIKOLAYEV, N. I. REVINA and V. M. ROZENBERG, *Fiz. Metal. Metalloved* **40** (1975) 1240.
8. K. TOMAN, *Acta Crystallogr.* **5** (1952) 329.
9. K. E. EASTERLING and P. R. SWANN, *Acta Metall.* **19** (1971) 117.
10. G. R. WOOLHOUSE, *Phil. Mag.* **28** (1973) 65.
11. G. CLIFF, D. J. POWELL, R. PILKINGTON, P. E. CHAMPNESS and G. W. LORIMER, in Electron Microscopy and Analysis, Institute of Physics Conference Series **68** (1983) p. 63.
12. W. BONFIELD and B. C. EDWARDS, *J. Mater. Sci.* **9** (1974) 398.
13. R. J. RIOJA and D. E. LAUGHLIN, *Acta Metall.* **28** (1980) 1301.
14. S. A. LOCKYER, PhD thesis, University of Liverpool (1992).

Received 17 November 1992
and accepted 11 March 1993